

## Electrical and mechanical properties of distorted carbon nanotubes

Alain Rochefort

*Centre de Recherche en Calcul Appliqué (CERCA), 5160 Boulevard Décarie, Bureau 400, Montréal, Québec, Canada H3X 2H9*

Phaedon Avouris

*IBM Research Division, T.J. Watson Research Center, P.O. Box 218, Yorktown Heights, NY 10598*

Frédéric Lesage

*Centre de Recherche Mathématiques (CRM), Université de Montréal, Case Postale 6128, Succursale Centre-Ville, Montréal, Québec, Canada H3C 3J7*

Dennis R. Salahub

*Département de Chimie, Université de Montréal, Case Postale 6128, Succursale Centre-Ville, Montréal, Québec, Canada H3C 3J7 and Centre de Recherche en Calcul Appliqué (CERCA), 5160 Boulevard Décarie, Bureau 400, Montréal, Québec, Canada H3X 2H9*

(Received 28 April 1999; revised manuscript received 3 August 1999)

We have calculated the effects of structural distortions of armchair carbon nanotubes on their electronic and electrical properties. We found that the bending of the nanotubes decreases their transmission function in certain energy ranges and leads to an increased electrical resistance. Electronic structure calculations show that these energy ranges contain localized states with significant  $\sigma$ - $\pi$  hybridization resulting from the increased curvature produced by bending. Twisting strongly affects the electronic structure of nanotubes (NTs). Normally metallic armchair ( $n,n$ ) NT's develop a band gap which initially scales linearly with twisting angle and then reaches a constant value. This saturation is associated with a structural transition to a flattened helical structure. The computed values of the twisting energy and of the band gap are strongly affected by allowing structural relaxation in the twisted structures. Finally, our calculations show that the large contact resistances observed for single-wall NT's are likely due to the weak coupling of the NT to the metal in side bonded NT-metal configurations. [S0163-1829(99)02943-4]

### I. INTRODUCTION

Carbon nanotubes (NT's) can be metallic or semiconducting. They have high mechanical strength and good thermal conductivity,<sup>1</sup> properties that make them potential building blocks of a new, carbon-based, nanoelectronic technology.<sup>2-5</sup> Conduction in defect-free NT's, especially at low temperatures, can be ballistic, thus involving little energy dissipation within the NT.<sup>6</sup> Furthermore, NT's are expected to behave like quasi-one-dimensional systems (Q1D) with quantized electrical resistance, which, for metallic armchair nanotubes at low bias, should be about  $6 \text{ k}\Omega$  ( $h/4e^2$ ). The experimentally observed behavior is, however, quite different. The contact resistance of single-wall nanotubes with metal electrodes is generally high, and at low temperatures, localization of the wave function in the nanotube segment contained between the metal electrodes is observed leading to Coulomb blockade phenomena.<sup>7</sup> This suggests that a barrier or band gap develops along the NT near its contact with the metal. Structural deformations are frequently observed in scanning tunneling microscope and atomic force microscope images of NT's, particularly in the vicinity of the metal electrodes. In an effort to understand the role of these deformations, we have used Green's function techniques to calculate the effects of bending and twisting of the NT's on their electronic structure and electric transport properties. We have also investigated the dependence of the contact resistance on the strength of the NT-metal pad interaction.

Most discussions of the electronic structure of NT's assume perfect cylindrical symmetry. However, this picture of a NT as a straight, geometrically and atomically perfect tube is somewhat oversimplified. Images of NT's quite often reveal structural deformations such as bent,<sup>8</sup> twisted,<sup>9</sup> or collapsed<sup>10</sup> tubes. These deformations may develop during growth, deposition, and processing, or following an interaction with surface features such as electrodes, or other NT's. An investigation of the electronic structure of weakly distorted nanotubes has been performed using a low energy field theory description.<sup>11</sup> The introduction of point defects such as vacancies<sup>12</sup> or disorder<sup>6,13</sup> has been shown to lead to significant modification of their electrical properties. AFM experiments<sup>14</sup> and molecular mechanics simulations<sup>15</sup> have shown that the van der Waals forces between NT's and the substrate on which they are placed can lead to a significant deformation of their structure. To maximize their adhesion energy NT's tend to follow the topography of the substrate<sup>14,15</sup>. Thus, for example, NT's bend to follow the curvature of the metal electrodes on which they are deposited. When the strain due to bending exceeds a certain limit, kinks develop in the nanotube structure.<sup>13,16,17</sup> It is important to understand how these NT deformations affect the electrical transport properties of the NT's. Could they be, for example, responsible for the low-temperature localization observed?<sup>7</sup> Early theoretical work on this issue was based on a tight-binding model involving only the  $\pi$  electrons of the NT's, and accounted for the electronic structure changes in-

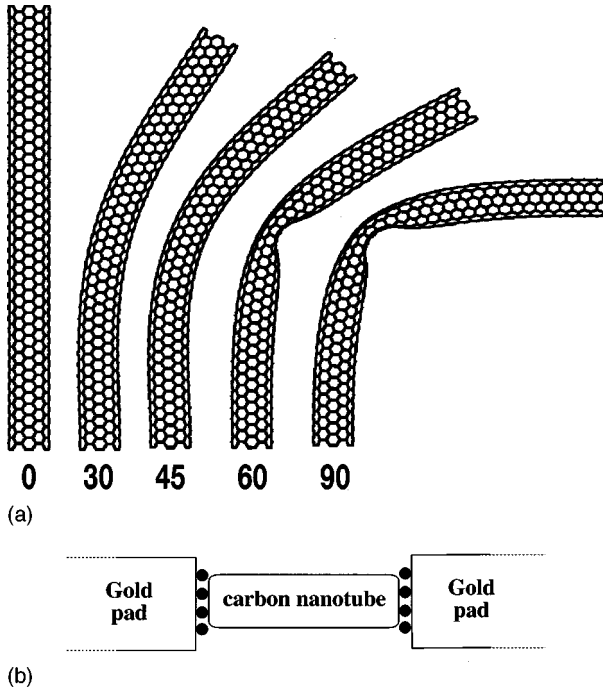


FIG. 1. (a) Structures of the isolated bent nanotubes used in the computation. The indices refer to the bending angles (in degrees). (b) Schematic of the model used in computation involving a finite length carbon nanotube contained between infinite gold pads.

duced by bending through the changes in  $\pi$ -orbital overlap at neighboring sites. This study concluded that bending distortions would have a negligible effect on the electrical properties of the NT's.<sup>11</sup> The applicability of this approach is limited to weak distortions. Experiments, however, show that strong deformations and kinks are common. Under such conditions, bending-induced  $\sigma$ - $\pi$  mixing, which was not considered before, becomes very important in strongly bent NTs<sup>18</sup>. In this work, the NT electronic structure is computed using the extended Hückel method<sup>19</sup> (EHM) that includes both  $s$  and  $p$  valence electrons. We have previously<sup>20</sup> shown that EHM calculations on an armchair (6,6) NT model (96 Å long) reproduce the electronic properties obtained with more sophisticated *ab initio* and band-structure computations on NT's. The approach we used in the computation of the electrical properties is similar to that of Datta *et al.*<sup>21,22</sup>

## II. COMPUTATIONAL DETAILS

The nanotube model used in the computations contains 948 carbon atoms arranged in an armchair (6,6) structure. The energetics of the deformations were determined with molecular mechanics using the TINKER program<sup>23</sup> with a modified MM3 force field.<sup>18</sup> Calculations were also performed using a tight-binding density-functional theory (TB-DFT) method developed by Porezag *et al.*<sup>24</sup> In both types of calculations the dangling bonds at the ends of the tubes were saturated by hydrogen atoms. The bond distance between carbon atoms in nondeformed regions of the NT is fixed to that in graphite 1.42 Å, leading to a tube length of 96 Å. The building of bent NT's using molecular mechanics minimization schemes<sup>25,23</sup> has been described in detail elsewhere.<sup>18</sup> The structures of the bent NT's are shown in Fig. 1(a). The

twisted structures were generated by two different schemes. In the first, continuous twisting, the circular plane sections of carbon atoms along the tube axis were rotated sequentially by an (additive) specified angle. In the second, alternate twisting, a (nonadditive) rotation was performed on every second section. The molecular mechanics calculations showed that it is less energetically demanding to continuously twist the tube than to twist it alternatively. Therefore, we will focus our attention on continuous deformations.

The electronic structures of distorted NT's were determined using the extended Hückel method (EHM).<sup>19</sup> EHM gives results similar to those obtained on extended NT's with more sophisticated methods.<sup>20</sup> The energy band gap was obtained as the difference between the highest occupied molecular orbital (HOMO) and lowest unoccupied molecular orbital (LUMO) energies. The metallic contacts consist each of 22 gold atoms in a (111) crystalline arrangement. The height of the NT over the gold layer is 1.0 Å, where the Au-C bond distances vary from 1.1 to 1.6 Å.

The conductance through a molecule or an NT cannot be easily computed; even if the electronic structure of the free molecule or NT is known, the effect of the contacts on it can be substantial<sup>26</sup> and needs to be taken into account. Typically, there will be two (or more) leads connected to the NT. We model the measurement system as shown in Fig. 1(b). The leads are macroscopic gold pads that are coupled to the ends of the NT through matrix elements between the Au surface atoms and the end carbon atoms of the NT. In most experiments to date the NT's are laid on top of the metal pads. As discussed above, the NT's then tend to bend around the pads. Such bending deformations are modeled in our calculations by introducing a single bend placed at the center of the tube. The electrical transport properties of a system can be described in terms of the retarded Green's function.<sup>21,27</sup> To evaluate the conductance of the NT we need to compute the transmission function,  $T(E)$ , from one contact to the other. This can be done following the Landauer-Büttiker formalism as described in Ref. 21. The key element of this approach lies in the treatment of the infinite leads which are here described by self-energies. We can write the Green's function in the form of block matrices separating explicitly the molecular Hamiltonian. After some simplification we obtain

$$G_{NT} = [ES_{NT} - H_{NT} - \Sigma_1 - \Sigma_2]^{-1}, \quad (1)$$

where  $S_{NT}$  and  $H_{NT}$  are the overlap and the Hamiltonian matrices, respectively, and  $\Sigma_{1,2}$  are self-energy terms that describe the effect of the leads. They have the form  $\tau_i^\dagger g_i \tau_i$  with  $g_i$  the Green's function of the individual leads<sup>22,28</sup> and  $\tau_i$  is a matrix describing the interaction between the NT and the leads. The Hamiltonian and overlap matrices are determined using EHM for the system gold-NT-gold. The transmission function,  $T(E)$ , that is obtained from this Green's function is given by<sup>21</sup>

$$T(E) = T_{21} = \text{Tr}[\Gamma_2 G_{NT} \Gamma_1 G_{NT}^\dagger]. \quad (2)$$

In this formula, the matrices have the form

$$\Gamma_{1,2} = i(\Sigma_{1,2} - \Sigma_{1,2}^\dagger). \quad (3)$$

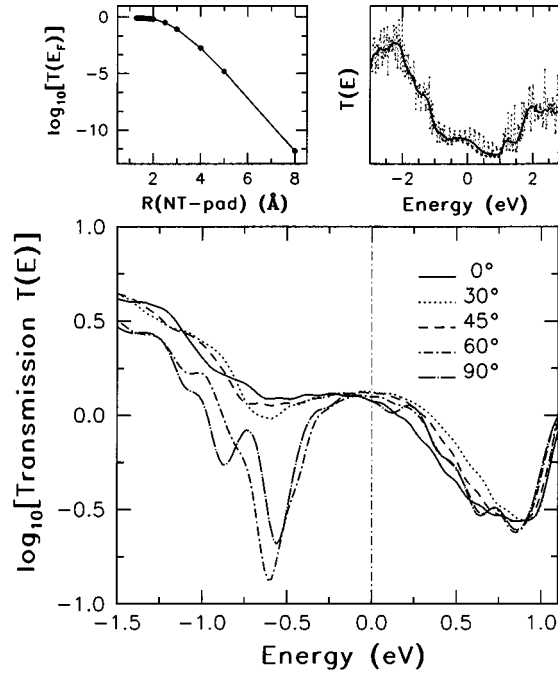


FIG. 2. Transmission function  $T(E)$  for the different bent nanotubes. The upper-right inset gives the raw data obtained from the computation for the straight NT along with the smoothed curve. The upper-left inset shows the variation of the transmission function  $T(E_F)$  with the nanotube-pad distance  $[R(\text{NT-pad})]$ . In this last figure, one gold-NT distance is fixed at  $1.0 \text{ \AA}$  while the other is varied.

The summation over all conduction channels in the nanotube allows the evaluation of the resistance at the Fermi energy,  $R = h/[2e^2T(E_F)]$ . Transport in the presence of an applied potential is also computed. The differential conductance is obtained in this case using the approximation<sup>21</sup>

$$\kappa(V) = \frac{\partial I}{\partial V} \approx \frac{2e^2}{h} [\eta T(\mu_1) + (1 - \eta)T(\mu_2)]. \quad (4)$$

In Eq. (4),  $\eta = V_{NT}/V$  where  $V_{NT}$  is the average electrostatic potential of the nanotube.  $\eta$  is used to describe how the electrostatic potential  $V$  is divided between the two junctions.<sup>22</sup> As a reference, we use the  $E_F$  obtained from EHM for individual nanotubes as the zero of energy.

### III. RESULTS AND DISCUSSION

#### A. Nanotube bending

In Fig. 2 we present the computed transmission function  $T(E)$  for the bent tubes [note that  $T(E)$  represents the sum of the transmission probabilities over all contributing NT conduction channels]. The upper-right figure of Fig. 2 shows the raw transmission results obtained for the straight NT. The fast oscillations of  $T(E)$  are due to the discrete energy levels of the finite segment of the carbon nanotubes used. For clarity, we will use smoothed curves in the description of the results. At  $E_F$ ,  $T(E)$  is about 1.2, leading to a resistance ( $\approx 11 \text{ k}\Omega$ ) higher than expected for ballistic transport [ $\approx 6 \text{ k}\Omega$  for  $T(E) = 2.0$ ]. This reduction in transmission is due to the contribution from the contact resistance. The in-

creasing  $T(E)$  at higher binding energies is due to the opening of new conduction channels. The asymmetry in the transmission  $T(E)$  is a function of the NT-pad coupling (C-Au distance). A longer NT-Au distance increases the  $T(E)$  above  $E_F$ , while it decreases it below  $E_F$ , and vice versa. Since the NT-pad geometry is kept fixed in all computations, this behavior does not obscure the effects induced by NT bending.

According to our calculation the contact resistance at  $E_F$  is only about  $5 \text{ k}\Omega$ , much smaller than the  $\approx 1 \text{ M}\Omega$  resistance typically observed in experiments on single-wall NT's<sup>2,5</sup>. The dependence of  $T(E)$  and contact resistance at  $E_F$  on the Au-NT distance is shown in the upper-left part of Fig. 2. We see that  $T(E_F)$  remains nearly constant between  $1\text{--}2 \text{ \AA}$ , then decreases exponentially. For distances appropriate for van der Waals bonding ( $\geq 3 \text{ \AA}$ ) the contact resistance is already in the  $\text{M}\Omega$  range. The above findings suggest that the high NT contact resistance observed experimentally may, in addition to experimental factors such as the presence of asperities at the metal-NT interface, be due to the topology of the contact. In most experiments, the NT is laid on top of the metal pad. The NT is at nearly the van der Waals distance away from the metal surface, and given that transport in the NT involves high  $k$  states, which decay rapidly perpendicular to the tube axis, the coupling between NT and metal is expected to be weak.<sup>29</sup> Direct chemical bonding between metal and NT should lead to a much stronger coupling. In this respect, it has been found<sup>30</sup> that high-energy electron irradiation of the contacts leads to a drastic reduction of the resistance. Since the irradiation is capable of breaking NT C-C bonds it may be that the resulting dangling bonds lead to a stronger metal-NT coupling.

The strongest modification of  $T(E)$  as a result of bending is observed at around  $E = -0.6 \text{ eV}$  where a transmission dip appears. This dip is strongest in the  $60^\circ$  bent NT. Furthermore, its transmission function at higher binding energies is lower than those of the  $0^\circ\text{--}45^\circ$  bent NT's, indicating that the transmission of higher conduction channels is also decreased. The nature of the dip at about  $-0.6 \text{ eV}$  can be understood by examining the local density of states (LDOS) of bent tubes shown in Fig. 3.<sup>18</sup> A change (increase) in the LDOS is seen in the same energy region ( $0.5\text{--}0.8 \text{ eV}$  below  $E_F$ ) as the transmission dip. This change is essentially localized in the vicinity of the deformed region. The new states result from the mixing of  $\sigma$  and  $\pi$  levels, have a more localized character than pure  $\pi$  states leading to a reduction of  $T(E)$ . As Fig. 3 shows, the change in transmission with bending angle is not gradual; the transmission of the  $30^\circ$  and  $45^\circ$  models is only slightly different from that of the straight tube. Apparently, large changes in DOS and  $T(E)$  require the formation of a kink in the NT structure, as is the case in the  $60^\circ$  and  $90^\circ$  bent NT's.

Once the transmission function is computed, the differential conductance or resistance can be easily determined for a given electrostatic potential profile. Figure 4 shows the results for two extreme cases of equilibration of the Fermi levels. The first is when  $\eta = 0$  [Fig. 4(a)], and the symmetric case  $\eta = 0.5$  [Fig. 4(b)]. When  $\eta = 0.0$ , the electrochemical potential of the NT matches that of one of the electrodes and the conductance spectrum is directly proportional to  $T(E)$ . This potential profile is appropriate in the case where one of

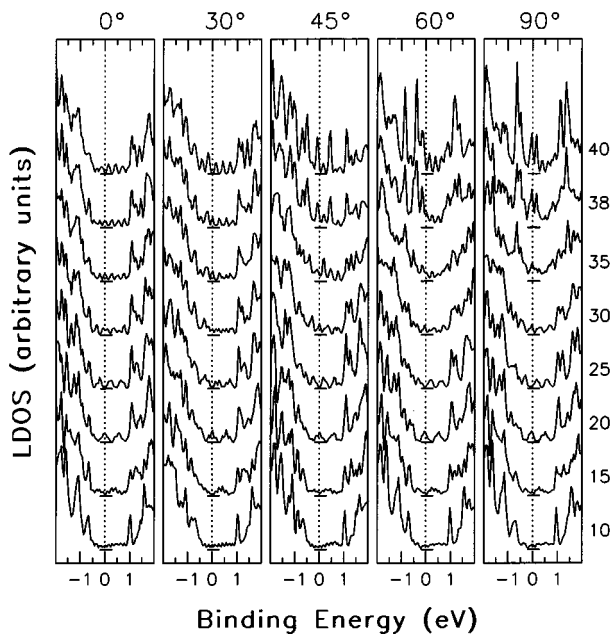


FIG. 3. Variation of the LDOS near the Fermi level for several bent (6,6) armchair nanotubes. (resolution = 0.05 eV). Indices give the relative position of the section in the nanotube structure (1: boundary; 40: middle of the nanotube).

the electrodes is weakly coupled to the NT, as when the NT is probed with an STM tip. As expected, there is no large difference between the 0°, 30°, and 45° models, while the 60° and 90° models show the dip structure at around 0.6 V. The nonlinear resistance (NLR) spectra show clearly a sharp increase by almost an order of magnitude at 0.6 V. These features are also observed when  $\eta=0.5$ , where the Fermi level of the NT is floating at half the voltage applied between the two gold pads. This value of  $\eta$  is more appropriate for

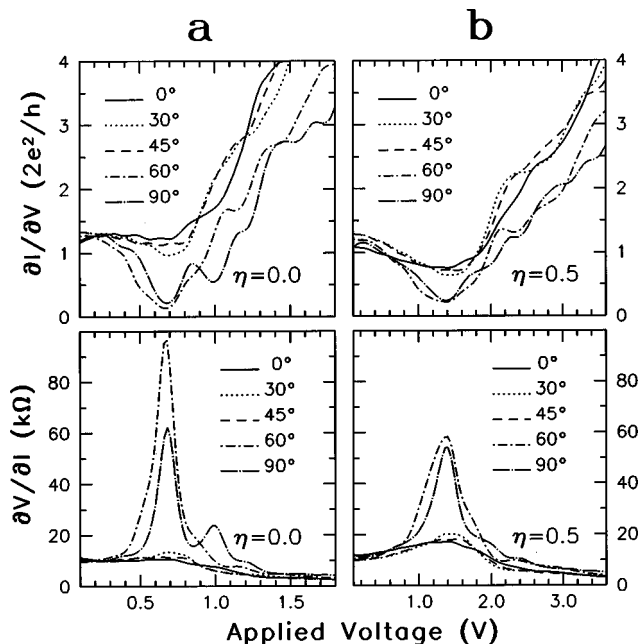


FIG. 4. Differential conductance (top) and resistance (bottom) of bent tubes for two extreme cases where (a)  $\eta=0.0$  and (b)  $\eta=0.5$ .

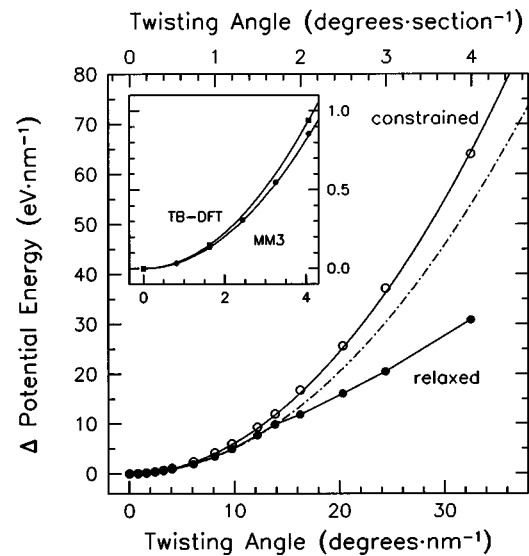


FIG. 5. Molecular mechanics calculation of the energy required to twist a (6,6) armchair NT as a function of twist angle, for a constrained (open circles) and a relaxed geometry (closed circles). The dot-dashed line corresponds to the quadratic law determined from the low twisting angle region of the relaxed NT. The inset shows a comparison of the MM3 and TB-DFT energies for small twisting angles.

the strong and symmetric electrode-NT-electrode coupling illustrated in Fig. 1(a). A broader conductance dip appears at about 1.2 V, and the NLR of the 60° bent tube increases by about a factor of 4 from the computed resistance of the straight tube. These results indicate that there exists a critical bending angle (between 45° and 60°) above which the conduction in armchair carbon nanotubes is drastically altered.<sup>31</sup>

## B. Nanotube twisting

We now consider the modifications of the atomic and electronic structure brought about by twisting an NT. In Fig. 5, we plot the potential energy for a continuous twisting deformation against the twist angle for a constrained (6,6) structure, and for a relaxed one where only the first two carbon sections at each end of the tube were held fixed. In the inset, we compare the energies obtained with molecular mechanics for small angle twisting of the relaxed structures to the energies determined with the TB-DFT method. A number of observations can be made. First, the energy required for even a moderate twisting of the tube is very large. At low twisting angles (inset) a quadratic law is obeyed. The twisting energies calculated using the MM3 potentials are lower than those computed using TB-DFT (inset). Therefore, in the following we will consider the MM3 energies as lower limits to the energetics of twisting deformations. Figure 5 shows clearly that structural relaxation has a very strong effect on the potential energy of deformation, especially for large twisting angles where the relaxation energy is computed to be of about the same order of magnitude as the final energy. Furthermore, the energy profile of the relaxed structure deviates from the quadratic law (dot-dashed line) for  $\Theta_T > 14^\circ \text{ nm}^{-1}$ . This deviation corresponds to the onset of a structural transformation where the tube flattens and takes on a helical shape [such as in Figs. 6(c) and 6(d)]. A similar

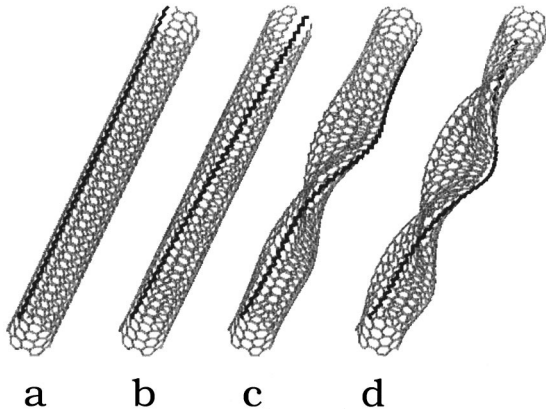


FIG. 6. Relaxed NT structures obtained with force-field MM3 energy minimization on 0 (a), 1 (b), 2 (c), and 3°section<sup>-1</sup> (d) twisted models.

transition has been observed in molecular dynamics simulations.<sup>32</sup> In order to determine the effect of the diameter on the collapsing of the nanotubular structures, we have also computed MM3 energies of twisted (10,10) models. Taking into account the differences in the number of carbon atoms involved ((10,10)/(6,6)=1.67), and the NT diameters ( $\phi_{(10,10)}/\phi_{(6,6)}=1.67$ ), we find that the energy needed to twist a (10,10) NT is similar to that needed to twist a (6,6) NT. The collapse of the (10,10) tubular structure into the helical shape occurs at a lower twisting angle than the (6,6) structure, i.e. when  $\Theta_T > 10^\circ \text{ nm}^{-1}$ . However, due to its larger diameter, the relative displacement of the carbon atoms during the tube to helix transition for a (10,10) NT is larger than in the case of a (6,6) NT.

Our calculations show that the twisting energies scale nearly linearly with the length of the nanotube. Therefore, we can extrapolate and obtain the twisting energies of longer nanotube segments, and use these energies to evaluate their Boltzmann distributions as a function of temperature. The relative population of twisted (6,6) structures can be described by

$$F(\Theta_T) = \exp\left[-\alpha \frac{L\Theta_T^2}{T}\right], \quad (5)$$

where,  $\alpha$  is a constant equal to  $580 \text{ nm} \cdot \text{deg}^{-2} \cdot \text{K}$ ,  $L$  is the nanotube length in nm,  $\Theta_T$  is the twisting angle (in  $\text{deg} \cdot \text{nm}^{-1}$ ), and  $T$  is the temperature. From this equation, it is clear that large twists cannot be generated by thermal excitation. For example, to obtain by thermal excitation a relatively small population (1%) of a  $1 \mu\text{m}$  long (6,6) nanotube twisted by  $9.8^\circ \text{ nm}^{-1}$ , which is equivalent to the twist deformation reported by Clauss *et al.* from STM images of nanotube ropes,<sup>9</sup> it would require a temperature larger than  $10^6 \text{ K}$ ! We conclude then that large scale nanotube twists must be the result of either mechanical interactions taking place during the deposition or manipulation of the nanotube sample, or they are introduced during the high-energy growth processes and frozen in place by shear forces due to the interaction with the substrate and other tubes. Local twisting associated with tube collapse is, however, less energetically demanding and is encountered quite often in AFM images.

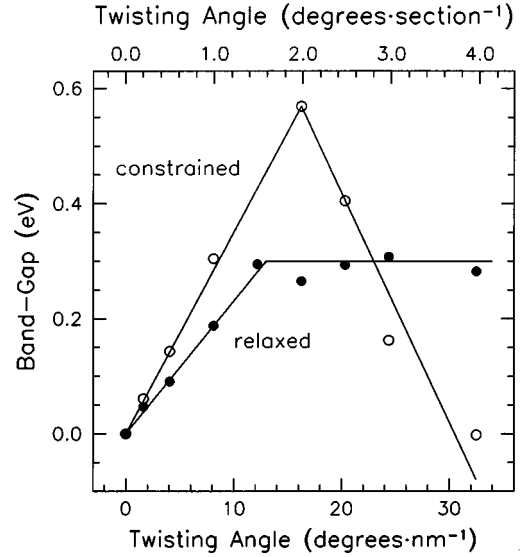


FIG. 7. Band-gap opening in a (6,6) nanotube as a function of the twist angle for a constrained geometry (open circles), and a relaxed geometry (filled circles).

The most important modification of the electronic structure induced by twisting a metallic armchair nanotube is the opening of a band gap. Figure 7 shows the variation of the band-gap value of a twisted (6,6) nanotube as a function of the twisting angle, for both constrained and relaxed NT structures. We find that for the constrained structure, the band gap increases linearly with twisting angle up to  $16^\circ \text{ nm}^{-1}$ , then gradually decreases to zero at higher angles. Allowing relaxation in the twisted nanotube structure has a strong influence on the value of the band gap; the gap increases linearly (but with a different slope) with twisting angle up to  $14^\circ \text{ nm}^{-1}$ , then reaches a stable value ( $\approx 0.3 \text{ eV}$ ) at higher angles. The first, linear, region corresponds to the opening of a gap produced by the straining, i.e., compression and dilatation of C-C bonds along the axis of the tube, brought about by twisting. The initial linear increase obtained in constrained structures is in general agreement with the predictions of low-energy theory<sup>11</sup> which, however, does not take relaxation into account. For higher twisting angles, the band-gap decrease observed for the constrained geometry is mainly due to the presence of strong interaction between destabilized  $\sigma$  and  $\pi$  orbitals near the Fermi level. The plateau observed in relaxed structures is the result of the collapse of the tubular structure into a flattened helix shape which decreases the large repulsive overlap of strained NT's [Figs. 6(c) and 6(d)].

The opening of a band gap in originally metallic nanotubes leads to a drastic modification of the electrical properties of nanotubes upon twisting by even low angles. In order to investigate the conduction of electrons in twisted (and relaxed) (6,6) nanotubes, we have connected both tube ends (with dangling bonds on the end carbons) to gold electrodes. Figure 8 shows the transmission  $T(E)$  spectra of nanotubes twisted by 0, 1.6, 4.1, and  $8.1^\circ \text{ nm}^{-1}$  angles (main panel). All these deformed tubes lie within the linear regime of the band-gap variation with twist angle. The variation of  $T(E)$  at  $E_F$  with twisting angle is shown at the upper-left panel, while the corresponding change in resistance at zero bias

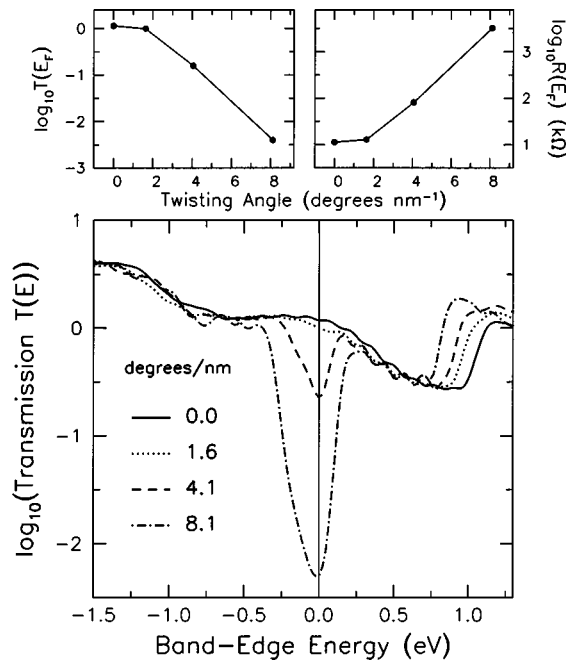


FIG. 8. Computed transmission function of a twisted (6,6) NT. The upper-left inset shows the logarithmic decay of  $T(E_F)$  with twisting angle, and the upper-right inset gives the variation of the resistance at zero bias for the same twisted NT.

[ $= 12.9 \text{ k}\Omega/T(E_F)$ ] is given at the upper-right panel. Twisting induces important changes in the  $T(E_F)$ , a property that determines the linear conductance of the system. Already a twist of  $4^\circ \text{ nm}^{-1}$  (or  $0.5^\circ/\text{section}^{-1}$ ), reduces the transmission by a factor of 14. It is interesting, however, that essentially no change is seen in  $T(E_F)$  at low twisting angles ( $< 2^\circ \text{ nm}^{-1}$ ) despite the fact that a finite band gap ( $\approx 0.04 \text{ eV}$ ) is calculated for the free NT. We attribute this behavior to the metal-induced gap states (MIGS) produced by the interaction of the short ( $96 \text{ \AA}$ ) NT segment with the gold metal electrodes<sup>33</sup> and the presence of charge-transfer doping. The MIGS tend to bridge the distortion-induced gap when the latter is small.<sup>34</sup> For twisting angles larger than  $2^\circ \text{ nm}^{-1}$ , the transmission decreases exponentially (see the upper-left in Fig. 8). At  $8^\circ \text{ nm}^{-1}$ ,  $T(E_F)$  has been de-

creased by more than two orders of magnitude, and if we consider transport into a strongly twisted, helical shape nanotube [see Figs. 6(c) and 6(d)], the decrease in  $T(E)$  is about five orders of magnitude. A twisting-induced band gap is, most likely, responsible for the recently documented field-effect transistor action of a twisted, normally metallic multi-wall nanotube.<sup>5</sup>

#### IV. CONCLUSION

In conclusion, we have calculated the effects of structural distortions of armchair carbon nanotubes on their electrical transport properties. We found that bending of the nanotubes decreases their transmission function and leads to an increased electrical resistance. The effect is particularly strong at bending angles higher than  $45^\circ$  when the strain is strong enough to lead to kinks in the nanotube structure. The electronic structure calculations show that the reduction in  $T(E)$  is correlated with the presence at the same energy of localized states with significant  $\sigma$ - $\pi$  hybridization due to the increased curvature produced by bending. Resistance peaks at or near  $E_F$  caused by bending can lead to localization at low temperatures or anomalous electrical transport properties. Our calculations of the resistance (including the contact resistance) of a perfect NT end bonded to gold electrodes give a value close to  $h/2.4e^2$  instead of  $h/4e^2$ . This increase in resistance is due to the finite transmission of the contacts. The much larger contact resistances observed in many experiments on SWNT's are likely due to the weaker coupling of the NT to the metal when the NT is simply placed on top of the metal electrodes (this resistance, however, depends on the length of the contact). We predict that NT's end bonded to metal pads will have contact resistances of only a few  $\text{k}\Omega$ . Such low contact resistances will greatly improve the performance of NT-based devices and unmask the Q1D transport properties of NT's. Twisting a normally metallic armchair NT opens up a band gap which scales linearly with the twist angle up to a critical angle. Twisting above this angle leads to the collapse of the tubular structure and the formation of a flattened helix. The observed band gap is due to the asymmetric compression and dilatation of the C-C bonds along the NT.

<sup>1</sup>M. S. Dresselhaus, G. Dresselhaus, and P. C. Eklund, *Science of Fullerenes and Carbon Nanotubes* (Academic, San Diego, 1996).

<sup>2</sup>S. J. Tans, A. R. M. Verschueren, and C. Dekker, *Nature (London)* **393**, 49 (1998).

<sup>3</sup>M. Bockrath, D. H. Cobden, P. L. McEuen, N. G. Chopra, A. Zettl, A. Thess, and R. E. Smalley, *Science* **275**, 1922 (1997).

<sup>4</sup>P. G. Collins, A. Zettl, H. Bando, A. Thess, and R. E. Smalley, *Science* **278**, 100 (1997).

<sup>5</sup>R. Martel, T. Schmidt, H. R. Shea, T. Hertel, and Ph. Avouris, *Appl. Phys. Lett.* **73**, 2447 (1998).

<sup>6</sup>C. T. White and T. N. Todorov, *Nature (London)* **393**, 240 (1998).

<sup>7</sup>A. Bezryadin, A. R. M. Verschueren, S. J. Tans, and C. Dekker, *Phys. Rev. Lett.* **80**, 4036 (1998).

<sup>8</sup>T. Hertel, R. E. Walkup, and Ph. Avouris, *Phys. Rev. B* **58**, 870 (1998).

<sup>9</sup>W. Clauss, D. J. Bergeron, and A. T. Johnson, *Phys. Rev. B* **58**, 4266 (1998).

<sup>10</sup>N. G. Chopra *et al.*, *Nature (London)* **377**, 135 (1995).

<sup>11</sup>C. L. Kane and E. J. Mele, *Phys. Rev. Lett.* **78**, 1932 (1997).

<sup>12</sup>L. Chico, L. X. Benedict, S. G. Louie, and M. L. Cohen, *Phys. Rev. B* **54**, 2600 (1996).

<sup>13</sup>M. P. Anantram and T. R. Govidan, *Phys. Rev. B* **58**, 4882 (1998).

<sup>14</sup>T. Hertel, R. Martel, and Ph. Avouris, *J. Phys. Chem. B* **102**, 910 (1998).

<sup>15</sup>T. Hertel, R. E. Walkup, and Ph. Avouris, *Phys. Rev. B* **58**, 870 (1998).

<sup>16</sup>S. Iijima, C. Brabec, A. Maiti, and J. Bernholc, *J. Chem. Phys.* **104**, 2089 (1996).

- <sup>17</sup>M. R. Falvo, G. J. Clary, R. M. Taylor II, V. Chi, F. P. Brooks, Jr., S. Washburn, and R. Superfine, *Nature (London)* **389**, 582 (1997).
- <sup>18</sup>A. Rochefort, D. R. Salahub, and Ph. Avouris, *Chem. Phys. Lett.* **297**, 45 (1998).
- <sup>19</sup>G. Landrum, YAEHMOP (Yet Another Extended Hückel Molecular Orbital Package), Cornell University, Ithaca, NY, 1995.
- <sup>20</sup>A. Rochefort, D. R. Salahub, and Ph. Avouris, *J. Phys. Chem. B* **103**, 641 (1999).
- <sup>21</sup>S. Datta, *Electronic Transport in Mesoscopic Systems* (Cambridge University Press, Cambridge, U.K., 1995).
- <sup>22</sup>W. Tian, S. Datta, S. Hong, R. Reifengerger, J. I. Henderson, and C. P. Kubiak, *J. Chem. Phys.* **109**, 2874 (1998).
- <sup>23</sup>Y. Kong and J. W. Ponder, *J. Chem. Phys.* **107**, 481 (1997).
- <sup>24</sup>D. Porezag, Th. Frauenheim, Th. Köhler, G. Seifert, and R. Kaschner, *Phys. Rev. B* **51**, 12 947 (1995).
- <sup>25</sup>N. L. Allinger, Y. H. Yuh, and J.-H. Lii, *J. Am. Chem. Soc.* **111**, 8551 (1989).
- <sup>26</sup>N. D. Lang and Ph. Avouris, *Phys. Rev. Lett.* **81**, 3515 (1998).
- <sup>27</sup>E. N. Economou, *Green's Functions in Quantum Physics* (Springer-Verlag, New York, 1983).
- <sup>28</sup>D. A. Papaconstantopoulos, *Handbook of the Band Structure of Elemental Solids* (Plenum Press, NY 1986).
- <sup>29</sup>The coupling strength depends on the amount of charge transfer, i.e., the difference in the work functions of the NT and the metal, and the length of the contact.
- <sup>30</sup>A. Bachtold, M. Henny, C. Terrier, C. Strunk, C. Schönenberger, J.-P. Salvetat, J.-M. Bonard, and L. Forró, *Appl. Phys. Lett.* **73**, 274 (1998).
- <sup>31</sup>The assumption that the potential drops linearly across the NT is particularly drastic for highly bent models. In reality, in the highly deformed region, the voltage would drop in the vicinity of defects. This voltage drop near defects would decrease the transmission probability of the propagating electrons, and consequently emphasize the magnitude of the changes we have computed with our first assumption.
- <sup>32</sup>B. I. Yakobson, C. J. Brabec, and J. Bernholc, *Phys. Rev. Lett.* **76**, 2511 (1996).
- <sup>33</sup>V. Heine, *Phys. Rev. A* **138**, 1689 (1965).
- <sup>34</sup>F. Leonard and J. Tersoff (unpublished).